J Mater Sci (2011) 46:1153–1160
DOI 10.1007/s10853-010-4885-6

Understanding the influence of particle size on strain versus fatigue life, and fracture behavior of aluminum alloy composites produced by spray deposition

W. Li · Z. H. Chen · D. Chen · J. Teng · Li Changhao

Received: 1 July 2010 / Accepted: 30 August 2010 / Published online: 8 September 2010

Abstract The strain versus fatigue life and fracture behavior of spray-formed Al–Si composites reinforced with SiC particles of two different sizes were studied under total strain amplitudes. Both composites exhibit short low-cycle fatigue (LCF) which follows a Coffin-Manson relationship, and display cyclic hardening at all strain amplitudes. The LCF endurance of the composite with large particles is higher than that of composite containing small particles in the high strain amplitudes, however, at low strains the difference in fatigue endurance between the two composites decreased. Moreover, the decrease in particle size results in a higher degree of hardening at low and middle strains, but reduces the magnitude of hardening at highest strain. Fractographic analysis reveals that particle/matrix debonding is the main mechanism of failure in composite with small particles, while fracture and debonding of SiC particle are predominant in the large particle reinforced composite.

Introduction

Al–Si alloy composites possess low thermal expansion coefficient, high wear resistance and high strength to weight ratio. As a result, they have emerged as structural components for application in automotive and aerospace industries [1]. These composites are produced by several processing methods, such as stir casting, squeeze casting [2], powder metallurgy [3], and spray forming, etc. Amongst these methods, spray forming technique has drawn considerable research interest due to its scope of forming near-net shape product with a reduced number of process steps compared to the powder metallurgy. Apart from this, the process offers advantage of rapid solidification, such as refined equiaxed structure with negligible segregation, extension of the solid solubility limit [4], and wider compositional flexibility. With the engineering application of metal matrix composites (MMCs), the fatigue behavior will become critical in design, life-prediction and reliability analysis of the components made of these materials.

Since in general MMCs show a lower tensile ductility than their counterpart matrix materials [5], comprehensive study of the fatigue behavior of MMCs is essential for their design and application. It has been reported that the presence of reinforcement in MMCs degrades the low-cycle fatigue (LCF) characteristics when the MMCs are subjected to strain-controlled cyclic loading [6–9]. There are many factors belonging to reinforcement characteristics to affect the fatigue properties, such as the volume fraction, shape, size and dispersion of the reinforcement. Kaynak et al. [10] have reported that increasing the volume fraction of SiC particulates in cast Al–Si alloy promotes better high cycle fatigue life. Koh et al. [11] have shown that SiC-particulate reinforced Al–Si cast alloy containing higher volume fraction of SiC particles exhibits a more pronounced strain-hardening rate leading to shorter life at a given strain amplitude. The effects of SiC volume fraction and particle size on the fatigue behavior of powder metallurgy 2080 Al alloy have been investigated by Chawla et al. [12]. They find that increasing volume fraction (from 10 to 30%) and decreasing particle size (from 23 down to 5 μm) result in an increase in fatigue resistance. Han et al. [13] have pointed out that powder metallurgy SiC_p/Al composite displays cyclic softening while the unreinforced

W. Li (✉) · Z. H. Chen · D. Chen · J. Teng · L. Changhao
College of Materials Science and Engineering,
Hunan University, Changsha, Hunan 410082, China
e-mail: lwzzgjajie@126.com

matrix show cyclic hardening. In addition, the evolution of cyclic softening becomes faster when the particle size increases. Varma et al. [14] have recognized that the cyclic stress response behavior of the SiC_p/Al–Cu–Mg composites has strong dependence on the size of the reinforcement. And composite with finer size SiC particles shows higher degree of cyclic hardening. Despite the great number of investigations into the fatigue behavior of MMCs, the effect of particle size on LCF behavior of this kind of composites produced by spray deposition has been limited. Thus, it is necessary to carry out a fundamental research work in this respect. The purpose of the present study is to understand the effect of particle size on strain versus fatigue life and fracture behavior of spray-deposited SiC_p/Al composites.

Experimental procedure

The Al–Si alloy with a nominal composition of Al–7Si–0.3Mg–0.01Mn–0.01Cu (mass%) and its composite reinforced with 15 vol.%SiC particles were prepared by multilayer spray deposition technology, the details of which were mentioned in Ref. [15]. The composites with different nominal particle sizes of 4.5 and 20 μm were prepared, hereafter denoted in this paper as 4.5 μm SiC_p/Al–Si and 20 μm SiC_p/Al–Si, respectively. Then, the sprayed ingots were extruded at a ratio of 17.3 to provide a rectangular extrusion with 10×120 mm^2 cross-section at 450 °C. Both the composites and unreinforced alloy were machined with the loading axis parallel to the extrusion direction and solution treated at 535 °C for 2.5 h, quenched in water and then artificially aged at 160 °C to achieve the peak-aged condition for the matrix. The aging time was 7 h for the Al–Si alloy and 4.5 μm SiC_p/Al–Si composite, 11 h for 20 μm SiC_p/Al–Si composite.

The tensile specimens with a gauge length of 25 mm and a gauge diameter of 5 mm were made, according to ASTM standard E8. Strain-controlled LCF tests were performed on a computer-controlled servo hydraulic test machine, INSTRON 8871, according to ASTM E606 at room temperature, using specimens of 15 mm gauge length and 5 mm diameter. A sinusoidal waveform with total strain amplitudes ranging from 0.3 to 0.5% was applied. The tests were carried out at constant cyclic frequency of 0.03 Hz and the load ratio was $R = -1$. An axial 12.5 mm clip-on extensometer was attached to the test specimen for the purpose of monitoring total strain amplitude during fully reversed strain amplitude-controlled fatigue tests. At each strain level at least three specimens were tested. The fracture surfaces of specimens were examined by scanning electron microscope (SEM) to determine the predominant fracture modes.

Results

Microstructure and tensile properties

The optical micrographs of the Al–Si composites with initial average SiC_p sizes of ~4.5 and ~20 μm are shown in Fig. 1a and b, respectively. In general, there appears to be a reasonably uniform distribution of SiC_p reinforcement within the matrix. The SiC particles in both composites are partially aligned along the extrusion direction. This has also been confirmed by recent three-dimensional visualization of the microstructure obtained by serial sectioning technique [16]. Some clustering tendency is observed in the 4.5 μm SiC_p/Al–7Si composite and it decreases as the size of the particulates increases.

The tensile test is the basis of the fatigue test. The relationship between stress and strain can be used to predict the level of the relative cyclic stress–strain. As shown in Table 1, incorporation of the reinforcing particles promotes the elastic modulus 15.84–18.94%. For a given volume fraction, the fine particle reinforced composite has less

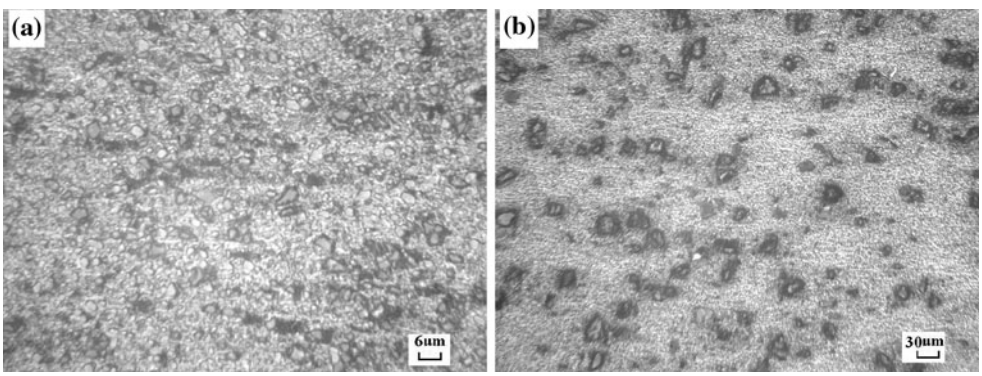

Fig. 1 Optical micrographs of longitudinal planes of the **a** 4.5 μm SiC_p/Al–Si composite, **b** 20 μm SiC_p/Al–Si composite

Table 1 Tensile mechanical properties of the Al–Si alloy and composites at room temperature

SiC content (vol.%)	SiC size (μm)	Elastic modulus, E (GPa)	0.2% proof strength, $\sigma_{0.2}$ (MPa)	Ultimate tensile strength, σ_b (MPa)	Elongation, A (%)
0	0	72.3	242.5	336.2	11.2
15	4.5	86.0	240.5	328.8	9.0
15	20	83.7	270.9	321.3	8.6

interparticle spacing as compared to the composite with large particles. Therefore, the reinforcements in the small particle composite probably share more portion of loading, giving rise to higher monotonic tensile strength and yield strength. In this case, the tensile strength of 4.5 μm SiC_p/Al–7Si composite is higher than that of 20 μm SiC_p/Al–7Si composite. These results are similar with the work of Han et al. [13], for a powder metallurgic Al alloy, containing 10 μm particles. However, Table 1 shows that the composite reinforced with 20 μm SiC_p has the largest yield strength. It does not fit the above relation that larger interparticle spacing in the 20 μm SiC_p reinforced composite, lower yield strength. It is reasonable to be thought that stress concentrations are generated around the clustering particles in fine particles composite leading to an earlier locally yield at relatively low loads.

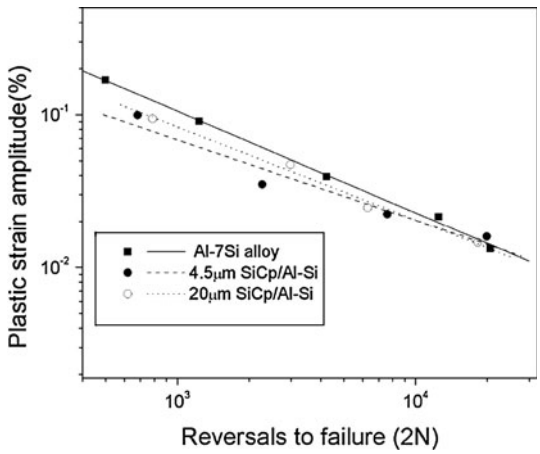

Fig. 2 Curves of plastic strain amplitude against number of reversals to failure for the matrix and composites tested at room temperature

Plastic-strain fatigue life

Plastic strain produces a number of damaging processes, which affects the microstructure, cyclic stress response and resultant LCF life during total strain amplitude-controlled cyclic deformation [17]. The LCF life of MMCs follows a Coffin-Manson relationship. Mathematically, Coffin-Manson relationship is described as:

$$\frac{1}{2}\Delta\varepsilon_p = \varepsilon_f'(2N_f)^c \quad (1)$$

where $2N_f$ is the reversal to failure, $\Delta\varepsilon_p$ is the plastic strain range. ε_f' and c are the fatigue ductility coefficient and fatigue ductility exponent, respectively. The plastic strain range can be determined from the cyclic hysteresis loop according to the following relation:

$$\Delta\varepsilon_p = \Delta\varepsilon_t - \frac{\Delta\sigma}{E} \quad (2)$$

where E is the Young's modulus, $\Delta\varepsilon_t$ is the total strain range, and $\Delta\sigma$ is the applied stress range.

Figure 2 represents the variation of fatigue life cycles with plastic strain amplitude for composites with various SiC_p sizes at a constant volume fraction. The parameters associated with LCF properties are listed in Table 2. It is obvious that the straight line for the Al–Si alloy is above the other two straight lines for the composites. Therefore, the Al–Si alloy has the best fatigue resistance. The absolute value of c for the Al–Si alloy is the highest and ε_f' is much larger than the 4.5 and 20 μm SiC_p/Al–Si composites. It can be seen that for the Al–Si alloy, the fatigue ductility coefficient, ε_f', is very close to the fracture strain in a monolithic tensile test. In strain control testing, a tendency of decrease in fatigue life with addition of reinforcement particles was also reported by Bonnen [18] in A2080-15 vol.%SiC, Koh et al. [11] in cast Al–Si–SiC composites and Han et al. [13] in powder metallurgy Al–20 vol.%SiC. In comparison with the results reported for the casting Al–Si/SiC composite by Rohatgi et al. [19], where the fatigue ductility exponent (c) and the fatigue ductility coefficient (ε_f') were −0.6066 and 0.0108, respectively, the fatigue resistance for SiC_P/Al–Si is better in this study because of the lower absolute value of c and higher ε_f' values. The tendency that spray-processed composite exhibits better cyclic-strain resistance than the as-cast composite is also reported in Ref. [20]. This is possibly attributed to the fine grain sizes, circular Si phases and uniform distribution of SiC particles present in sprayed materials.

It can be seen from Fig. 2 that the fatigue life differences between the matrix and the composites with particles of two different sizes depend strongly on the strain amplitude. The LCF endurance of the composite with large particles is higher than that of composite containing small particles in the high strain regions, however, at low strains the difference in fatigue endurance between the two composites decreased. In addition, the composite containing

Table 2 Low cycle fatigue parameters

SiC content (vol.%)	SiC size (μm)	Fatigue ductility coefficient, ε_f' (%)	Fatigue ductility exponent, c	Linear relational exponent
0	0	10.46	−0.6657	0.9986
15	4.5	2.63	−0.5284	0.9735
15	20	5.60	−0.6094	0.9950

large SiC particles exhibits a higher fatigue-ductility coefficient (ε_f') than the small particles composite. Similar with the observations reported in Ref. [13], the result from comparison between the two composites is that the composite with large particles shows a longer fatigue life at high plastic strain regions, but the composite containing small particles has a greater fatigue endurance at low strain amplitudes.

Cyclic stress response

The cyclic stress response curves of the Al–Si alloy and the two SiC_p/Al–Si composites under various total strain amplitudes at room temperature are shown in Fig. 3. The stress amplitude is taken as the average of the peak values of the stress in tension and in compression during cyclic loading. Unlike the results reported for MMCs and aluminum alloy matrix [13], the cyclic response of reinforced aluminum and the Al–Si alloy is similar to each other. All the matrix and the composites show evidence of initial hardening and the cyclic hardening rates for the composites are greater than that for the matrix at initial several hundred cycles for all total strain amplitudes. However, the Al–Si alloy shows a second hardening at strain amplitudes (0.35–0.5%), while a cyclic stable is observed at lowest strain amplitude (0.3%) after initial hardening. In contrast, the composites harden progressively to failure from onset of fully reversed cyclic deformation. In addition, Strain amplitude also affects the degree of cyclic hardening. The specimen subjected to a higher strain amplitude shows more cyclic hardening.

By comparing Fig. 3b with c, it is interesting to note that the increase in particle size results in a slow evolution cyclic hardening for a given strain amplitude. In order to highlight the effect of cyclic hardening as a function of applied total strain amplitude, the percentage degree of hardening $[(\Delta\sigma_n - \Delta\sigma_1)/\Delta\sigma_1 \times 100\%]$ is plotted with the applied total strain amplitude (%) in Fig. 4. Here, $\Delta\sigma_n$ and $\Delta\sigma_1$ are the stress range at half life and first cycle,

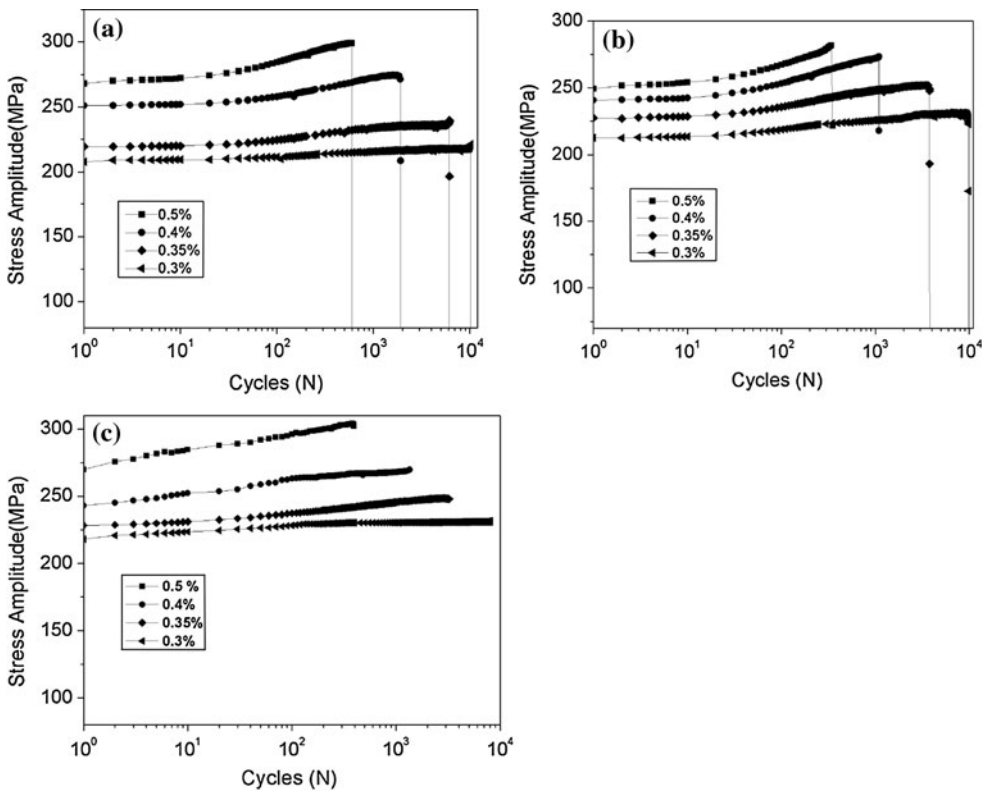

Fig. 3 Cyclic stress response curves for **a** the Al–Si alloy, **b** the 4.5 μm SiC_p/Al–Si composite, and **c** the 20 μm SiC_p/Al–Si composite

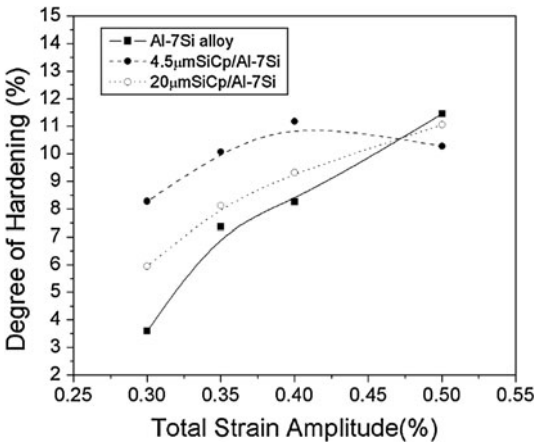

Fig. 4 Degree of hardening (%) as a function of total strain amplitude (%)

respectively. It is evident from Fig. 4 that the degree of cyclic hardening of 4.5 μm SiC_p/Al–Si composite is higher than those of 20 μm SiC particulates reinforced composite and matrix alloy, with applied total strain amplitudes (±0.3, ±0.35, and ±0.4%). However, it becomes lower than those of 20 μm SiC particulates reinforced composite and matrix alloy at the highest amplitude (±0.5%). In case of the Al–Si, the magnitude of the degree of hardening increases with increasing total strain amplitude at all the strain amplitudes. Moreover, it become higher than those of 4.5 and 20 μm SiC_p/Al–Si composite at the highest amplitude employed (±0.5%).

Furthermore, the finer particle reinforced composite results in less interparticle spacing, then share more portion of loading, giving rise to higher cyclic stress response. However, the experiment cyclic stress is not the case. The cyclic stress of the two composites is comparable at low strain amplitudes (0.3–0.4%). but it becomes higher in case of the composite with 20 μm particles than that of the 4.5 μm particles reinforced aluminum at the highest strain amplitude (±0.5%). One possible explanation is that the finer particles in this study result in clustering, which can easily initiate fatigue cracking because of the poor bonding between the clustering particles and the matrix.

Fracture behavior

Fatigue fractographs of the composites and unreinforced aluminum specimens are shown in Fig. 5. Fatigue striations and secondary cracks along the fatigue striations are observed on the fracture surface of the matrix as shown in Fig. 5a. Plenty of small dimples of 3–4 μm were due to the decohesion of Si particles in the Al–Si alloy during cyclic straining. No significant difference was observed in the fracture characteristics of unreinforced alloy at low strain (0.3%) and high strain (0.5%), Fig. 5a and b.

The fractographies of the composites are different from that of the unreinforced aluminum. Fatigue striations in composites are not obvious and most of them are covered by the SiC particles. On the fracture surface of the composite containing 4.5 μm SiC particles there are a population of unequiaxed dimples due to decohesion of SiC and Si particles as shown in Fig. 5c and d. The amount of SiC_p appeared on the fracture surface is less than that shown in Fig. 1a. Little of the SiC breakage is observed in Fig. 5c and d. It means that fine particles is not easy to break and the fracture surface had predisposition to avoid small SiC particles, which is similar to the LCF fracture surface features of the SiC_p/Al composite observed in Ref. [13]. In addition, it can also be seen from Fig. 5d that at the higher total strain amplitude of 0.5%, the fatigue cracks initiated at multisources only propagate for a small distance and rapidly through the matrix between the clusters of SiC particles under higher stress applied, then final fracture occurs due to the reduction of the effective loading area. For the 20 μm SiC_p/Al–Si composite the fracture surface contains the fracture and debonding of SiC particle shown in Fig. 5e and f. The number of SiC particles emerged on the fracture surface is close to that in Fig. 1b. The reason is that the large particles are hard to be avoided and considerably likely to break. Moreover, Fig. 5e and f also show that a higher fraction of particles were fractured in the large particle reinforced composite tested at high strain than at low strain.

Discussion

The effect of particle size on fatigue life

Usually, composites containing larger particles should exhibit worse fatigue properties than fine particles reinforced composite. The reasons for this behavior are that the larger reinforcement particles contain more defects, and the stress concentration is larger while a crack is propagating to a particle. So, it seems easier for a large particle to crack and for the crack to propagate. However, the experimental results obtained in this study and Han et al. [13] have both revealed that composite with large particles shows a longer fatigue life at high plastic strain regions, but the composite containing small particles has a greater fatigue endurance at low strain amplitudes. Reasonable explanation is discussed in terms of the different fracture modes at different strain amplitudes by Han et al. [13]. Under the high strain amplitude, where the contribution of monotonic modes of fracture dominates [21], the nucleation, growth and coalescence of voids play the major role in the fracture. The small SiC particles decohesion result in larger number of voids, then this kind of composite is easier to fail than big

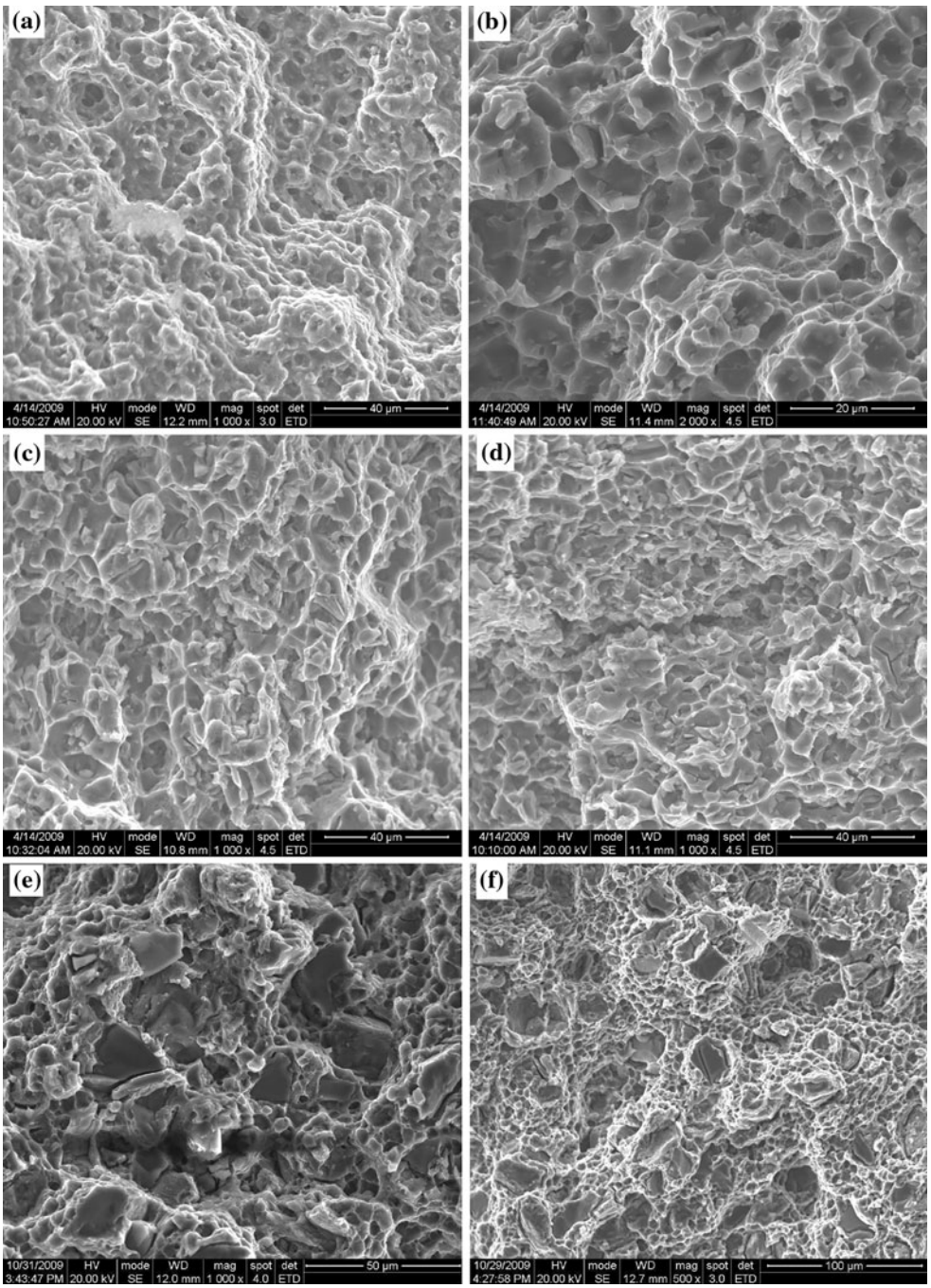

Fig. 5 SEM micrographs of fatigue fracture surfaces for the **a** Al–Si alloy, $\Delta\varepsilon_t/2 = 0.3\%$, **b** Al–Si alloy, $\Delta\varepsilon_t/2 = 0.5\%$, **c** 4.5 μm SiC_p/Al–Si composite, $\Delta\varepsilon_t/2 = 0.3\%$, **d** 4.5 μm SiC_p/Al–Si composite, $\Delta\varepsilon_t/2 = 0.5\%$, **e** 20 μm SiC_p/Al–Si composite, $\Delta\varepsilon_t/2 = 0.3\%$, and **f** 20 μm SiC_p/Al–Si composite, $\Delta\varepsilon_t/2 = 0.5\%$

particle composite at high strain amplitudes, thus leads to a shorter fatigue life. When low strain amplitudes are applied, fatigue endurance of the composites mainly depends on its strength. Small SiC particles are not easy to break. Therefore, the small particle reinforced composite has longer fatigue endurance at low strain ranges.

The effect of particle size on cyclic stress response

Based on the continuum theory, particle size should not affect cyclic hardening/softening. However, the results obtained in this study could not support the above viewpoint (as shown in Fig. 4). The differences in the

characteristics of cyclic hardening for the different composites and the matrix alloy under total strain amplitude are correlated with the conjoint and mutually interactive and competitive influences of hardening and softening, which occur simultaneously during fatigue process. Here the hardening is intrinsic for the matrix alloy Al–Si alloy, and the softening is due to initiation and growth or a large number of voids or microcracks in the entire stressed volume.

The hardening effect of the SiC_p/Al–Si is observed at the beginning of cyclic loading without any cyclic stable region, resulted from the pre-existing high dislocation density in the aluminum alloy matrix due to the presence of the brittle SiC_p reinforcements [22, 23]. Then, the dislocation density progressively increases with increasing number of strain cycles, due to the interaction of mobile dislocations with the brittle particles (SiC and Si) and more dislocation–dislocation interactions. Besides, the magnitude of dislocation density is strongly dependent on the particle size. Under the same amplitudes controlled condition, the degree of hardening would become higher in the 4.5 μm SiC_p/Al–Si composite due to the increase in dislocation density with decreasing reinforcement interparticle spacing as a result of reduced particle size [24], compared with 20 μm SiC_p/Al–Si composite.

The softening effect is attributed to the formation and presence of a number of microscopic cracks, their growth through the composite microstructure, and eventual coalescence to form one or more macroscopic cracks. The tendency toward softening is strongly dependent on the applied strain amplitude and microstructure characteristics. As mentioned in the "The effect of particle size on fatigue life" section, at lower strain amplitude, the larger particles in the 20 μm SiC_p/Al–Si composite have a higher probability of containing critical flaw, which generates high load transferring from the plastically deformed aluminum matrix to the elastically deformed particle, leading to their crack, the process of which is easier to occur compared to the 4.5 μm SiC_p/Al–Si composite. Therefore, the degree of cyclic hardening of 20 μm SiC_p/Al–Si is lower as compared to 4.5 μm SiC_p/Al–Si at ±0.3, ±0.35, and ±0.4% total strain amplitude, may be attributed to its relatively lower dislocation density and higher particle fracture. However, at highest strain amplitude (±0.5%), the softening effect for the 4.5 μm SiC_p/Al–Si composite is exacerbated by the rapid growth and coalescence of void once initiation has occurred in the composite due to the agglomeration of SiC particulates, therefore the hardening would be suppressed, which leads the decrease in observed degree of cyclic hardening. The cause of highest cyclic hardening for the Al–Si alloy at the highest total strain amplitude may be due to the relatively lowest voids only caused by Si decohesion.

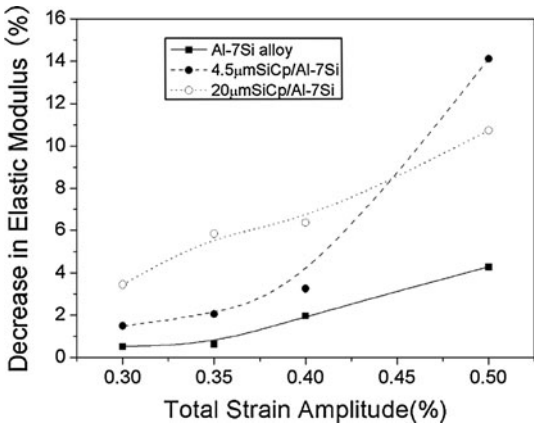

Fig. 6 Percentage decrease in elastic modulus of composites and matrix alloy with total strain amplitude

The percentage decrease in elastic modulus, with applied total strain amplitude is shown in Fig. 6. The decrease in modulus is calculated by subtracting the elastic modulus at half life with that before cycling. Composite with 20 μm SiC particles reveals significant decrease in the elastic modulus at total strain amplitudes (0.3–0.4%) as compared to that of 4.5 μm SiC particles composite. However, when the highest amplitude applied, the magnitude of decrease in elastic modulus of 20 μm SiC particles composite becomes smaller than that of fine particle composite. This indicates that the fraction of particle fracture and debonding during cycling for 20 μm SiC_p/Al–Si composite at low strain amplitudes is greater, while at highest strain amplitude the number of microcracks is smaller as compared to the 4.5 μm SiC_p/Al–Si composite, thus confirming the above hypothesis.

Conclusions

The LCF life and cyclic stress response behavior of the SiC_p/Al–Si composites used in this study have strong dependence on the size of the reinforcement.

(1) Both composites exhibit short LCF which follows a Coffin-Manson relationship. The fatigue ductility coefficient of the large particle composite ($\varepsilon_f' = 5.60$) is higher than that of the small particle reinforced composite ($\varepsilon_f' = 2.63$). The LCF endurance of the composite with large particles is higher than that of composite containing small particles in the high strain regions, however, at low strains the difference in fatigue endurance between the two composites decreased.

(2) All the composites and the matrix cyclically harden and the cyclic hardening rates for the composites are greater than that for the matrix at initial several

hundred cycles for all total strain amplitudes. However, the Al–Si alloy shows a second hardening at strain amplitudes (0.35–0.5%), and cyclic stable at lowest strain amplitude (0.3%) after initial hardening. In contrast, the composites harden progressively after the initial hardening for all strain amplitudes.

(3) The cyclic hardening response of the composite is dependent on the particle size of reinforcement and the cyclic strain amplitude. The decrease in particle size results in a higher degree of hardening at lower strain amplitudes, but reduces the magnitude of hardening at highest strain amplitude. Mechanisms responsible for this behavior are ascribed to concurrent and competing influences of the increase in hardening resulted from the increase in dislocation density with decreasing reinforcement interparticle spacing as a result of reduced particle size, and various rate of softening induced by fracture or debonding of the reinforcement particle depending on the strain amplitude.

(4) Fractographic analysis reveals that particle/matrix debonding is the main mechanisms of failure in the 4.5 μm SiC_p/Al–Si composite, while fracture and debonding of SiC particle are predominant in the 20 μm SiC_p/Al–Si composite.

Acknowledgements The authors are grateful to the international cooperation of Hunan province in China (project 2007WK2005) and National Natural Science Foundation (50875225).

References

1. Suresh S, Mortensen A (1997) Int Mater Rev 42:85
2. Sahin Y (2003) Mater Des 24:671
3. Wang F, Yang B, Duan XJ, Xiong BQ, Zhang JS (2003) J Mater Process Technol 137:191
4. Lavernia EJ (1991) Key Eng Mater 53-55:153
5. Mott G, Liaw PK (1988) Metall Mater Trans 19A:2233
6. Srivatsan TS (1992) Int J Fatigue 14:173
7. Levin M, Karlsson B (1993) Int J Fatigue 15:377
8. Srivatsan TS, Auradkar R (1992) Int J Fatigue 14:355
9. Llorca J, Suresh S, Needleman A (1992) Metall Mater Trans 23A:919
10. Kaynak C, Boylu S (2006) Mater Des 27:776
11. Koh SK, Oh SJ, Li C, Ellyin F (1991) Int J Fatigue 21:1019
12. Chawla N, Andres C, Jones JW, Allison JE (1998) Metall Mater Trans 29:2843
13. Han NL, Wang ZG, Sun LZ (1995) Scripta Metall Mater 33:781
14. Varma VK, Kamat SV, Mahajan YR (1998) Scripta Mater 38:1571
15. Chen ZH (2003) Multi-layer spray deposition technology applications, 1st edn. Hunan University Publications, Hunan, China
16. Chawla N, Ganesh VV, Wunsch B (2004) Scripta Mater 51:161
17. Lloyd DJ (1992) In: Arnberg L, Lohne O, Nes E, Ryum N (eds) The third international conference on aluminum alloys (ICAA3), vol III. Norwegian Institute of Technology, Trondheim, Norway, pp 145
18. Bonnen JJ, Allison JE, Jones JW (1991) Metall Mater Trans 22A:1007
19. Rohatgi PK, Alaraj S, Thakkar RB, Daoud A (2007) Composites Part A 38:1829
20. Srivatsan TS, Srivatsan TS, Lavernia EJ (1993) Compos Sci Technol 49:303
21. Kumai S, King JE, Knott JF (1992) Fatigue Fract Eng Mater Struct 15:1
22. Arsenault RJ, Wang L, Feng CR (1991) Acta Metall Mater 39:47
23. Sun ZM, Li JB, Wang ZG, Li WJ (1992) Acta Metall Mater 40:2961
24. Nan CW, Clarke DR (1996) Acta Mater 44:3801